Probabilistic Orientation Field Estimation for Fingerprint Enhancement and Verification

Kuang-chih Lee, Salil Prabhakar
DigitalPersona Inc.
720 Bay Road, Redwood City, CA 94587
{KuangL, SalilP}@digitalpersona.com

Abstract

We present a novel probabilistic method to estimate the orientation field in fingerprint images. Traditional approach based on the smoothing of local image gradients usually generates unsatisfactory results in poor quality regions of fingerprint images. We show how to improve the orientation field estimation by first constructing a Markov Random Field (MRF) and then inferring the orientation field from the MRF model. The MRF is made up of two components. The first component incorporates a global mixture model of orientation fields learned from training fingerprint examples. The second component enforces a smoothness constraint over the orientation field in the neighboring regions. The improved fingerprint orientation field is useful in fingerprint enhancement and minutiae extraction processes. We show remarkable improvement of fingerprint verification accuracy on a relatively large fingerprint dataset based on the proposed approach.

1. Introduction

Fingerprint recognition accuracy relies strongly on accurate extraction of fingerprint features. The two most prominent fingerprint features are ridge ending and bifurcations, collectively known as minutiae points. In order to extract precise minutiae information, an input fingerprint image generally needs to be enhanced by convolving with certain types of orientation-selective filters, such as Gabor or steerable filters, along the ridge flow orientation at each pixel/block location [1, 2]. Since these contextual filters are orientation selective, this process requires accurate estimation of orientation field.

In this paper, we show how to construct Markov Random Field (MRF) that improves the orientation field estimation in a principled way. Inference in the MRF searches the orientation space and tries to remove the spurious minutiae points. Our MRF representation discretizes the continuous orientation space by using a small number of actual training fingerprint examples to suggest possible hypotheses, which makes the inference process efficient. We show remarkable improvement of fingerprint verification accuracy on a relatively large fingerprint dataset based on the proposed approach.

2. Related Work

Traditional approaches usually extract the orientation flow directly by computing the intensity gradient from the input fingerprint image [3, 4, 5, 6]. The results are then commonly smoothed by some local averaging, diffusion, or voting methods in order to reduce the effects of noise [7, 8, 9]. These type of methods usually work fairly well for a large number of good quality fingerprint images, but we believe that they can be improved for poor quality fingerprint images.

A different approach that has been proposed for orientation field estimation is the model-based approach. Sherlock et al. [10] presented a so-called zero-pole model to estimate the fingerprint orientation topology based on global singular points (i.e., cores and deltas). One limitation of this approach is that the orientation fields are identical when any two fingerprints have the same singular points. Thus the model cannot account for all the natural variations of orientation fields. Further, this approach cannot handle arch type of fingerprints, which do not have singular points. Some extensions proposed by Zhou et al. [11] and Li et al. [12] combine the local gradient and the global point-charge model by interpolation of polynomial or piece-wise linear functions. However, the main limitation of these approaches is that they are dependent on reliable detection of singular points, which is extremely difficult when the singular points are located in the poor quality regions of fingerprint images.

Dass [13] proposed a Markov model to estimate fingerprint orientation fields and extract singularities. Our work bears some resemblance to this method in the sense that our method also admits a Markovian interpretation. However,

our algorithm incorporates a global mixture model of orientation fields learned from training examples, but Dass's approach only contains the quality and smooth pairwise priors. Therefore, Dass approach cannot recover the orientation field in very poor quality areas of fingerprint images.

Wang et al. [14] proposed a global model-based orientation field estimation approach by using low order 2D Fourier basis as a smooth prior to remove noise. This approach requires an initial estimate of the orientation field in order to compute the Fourier coefficients by solving a linear least square problem. The initial estimate is generally based on the gradient information. Starting from the noisy initial estimate, the orientation field cannot be recovered in very poor quality areas of fingerprint images based only on the smoothness prior.

3. Mathematical Framework

In this section, we describe how to incorporate a global mixture model of orientation fields learned from training fingerprint examples and the fingerprint image gradient information into a Markov Random Field (MRF). We also show how to perform inference in the MRF to yield more accurate orientation field.

Let I denote a grayscale fingerprint image, where $I(\mathbf{x})$ represents the intensity of the pixel at the location $\mathbf{x} = [x, y]^T$. We assume that the orientation field of the fingerprint ridge patterns can be represented by a discrete matrix, denoted by O, where each element $O(\mathbf{x}) \in [0, \pi]$ represents the local ridge orientation at pixel $\mathbf{x} = [x, y]^T$.

Our MRF is a representation of a joint probability distribution over the orientation variables O. Below we first describe the design of the MRF, and then we show how to discretize the continuous orientation space and perform inference efficiently.

3.1. MRF Model

We build the pairwise Markov network with the likelihood given in the following form:

$$P_\phi(O) = \frac{1}{Z} \prod_i \phi_i^q(O(\mathbf{x}_i)) \prod_{\mathbf{x}_i, \mathbf{x}_j \in \Omega} \psi_{ij}^c(O(\mathbf{x}_i), O(\mathbf{x}_j)), \tag{1}$$

where Z is a normalization constant, also called partition function, given by:

$$Z = \sum_O \prod_i \phi_i^q(O(\mathbf{x}_i)) \prod_{\mathbf{x}_i, \mathbf{x}_j \in \Omega} \psi_{ij}^c(O(\mathbf{x}_i), O(\mathbf{x}_j)), \tag{2}$$

which ensures that the probability distribution $P_\phi(O)$ given by Equation 1 is correctly normalized. Ω denotes the set of neighborhood pixel pairs. The problem of estimating the orientation field can be treated as the *maximum a posteriori* (MAP) inference problem in the Markov network:

$$O^* = \arg\max_O \; P_\phi(O). \tag{3}$$

The MRF is made up of two kinds of potentials: single quality potentials $\phi_i^q(O(\mathbf{x}_i))$, and pairwise consistent potentials $\psi_{ij}^c(O(\mathbf{x}_i), O(\mathbf{x}_j))$. The design of these potential functions focuses on how to express the idea of the quality estimation of the orientation field $O(\mathbf{x}_i)$. In the following subsections, we first describe how to measure the quality of the orientation field, and then present the mathematical formulation of the potential functions.

3.2. Steerable Filters

In order to estimate the quality of the orientation field $O(\mathbf{x}_i)$, first we compute a filtered image, $P(\mathbf{x}_i)$, by convolving the second order steerable filter pair $G_2(\theta)$ and $H_2(\theta)$, where $\theta = O(\mathbf{x}_i)$, with a local window $W(\mathbf{x}_i)$ at location $\mathbf{x}_i$ of the input fingerprint image I. G_2 and H_2 are computed by a linear combination of basis filters [15]:

$$\begin{aligned} G_2(\theta) &= \sum_{i=a,b,c} k_{2i}^G(\theta) G_{2i} \\ H_2(\theta) &= \sum_{i=a,b,c,d} k_{2i}^H(\theta) H_{2i}, \end{aligned} \tag{4}$$

where the set of basis filters G_{2i}, H_{2i} are X-Y separable, quadrature pair basis filters, and $k_{2i}^G(\theta), k_{2i}^H(\theta)$ are the weight coefficients specified as follows:

$$\begin{aligned} G_{2a} &= 0.9213(2x^2 - 1)e^{-(x^2+y^2)} \\ k_{2a}^G(\theta) &= \cos^2(\theta) \\ G_{2b} &= 1.843xye^{-(x^2+y^2)} \\ k_{2b}^G(\theta) &= -2\cos(\theta)\sin(\theta) \\ G_{2c} &= 0.9213(2y^2 - 1)e^{-(x^2+y^2)} \\ k_{2c}^G(\theta) &= \sin^2(\theta) \\ H_{2a} &= 0.9780(-.254x + x^3)e^{-(x^2+y^2)} \\ k_{2a}^H(\theta) &= \cos^3(\theta) \\ H_{2b} &= 0.9780(-.7515 + x^2)(y)e^{-(x^2+y^2)} \\ k_{2b}^H(\theta) &= -3\cos^2(\theta)\sin(\theta) \\ H_{2c} &= 0.9780(-.7515 + y^2)(x)e^{-(x^2+y^2)} \\ k_{2c}^H(\theta) &= 3\cos(\theta)\sin^2(\theta) \\ H_{2d} &= 0.9780(-.254y + y^3)e^{-(x^2+y^2)} \\ k_{2d}^H(\theta) &= -\sin^3(\theta) \end{aligned} \tag{5}$$

We need to emphasize the steerable property here. 'Steerable' means that the basis filters G_{2i}, H_{2i} are independent of the input orientation angle θ, and therefore, we

only need to convolve G_{2i}, H_{2i} with input fingerprint image once. The filtered image, P, used to estimate the quality of orientation fields can be iteratively updated by only re-calculating the coefficients k_{2i}^G, k_{2i}^H and steering the filter output accordingly. This is the main reason to choose steerable filter instead of Gabor filter in our framework because it is less expensive in iterative computation.

Let $*$ denote the convolution operator. The filtered image P can be finally computed by the following equation:

$$P(\theta, \mathbf{x}_i) = \arctan(\frac{H_2(\theta) * I(\mathbf{x}_i)}{G_2(\theta) * I(\mathbf{x}_i)}), \tag{6}$$

where $P(\theta)$ is the phase angle of the complex number $G_2(\theta) * I(\mathbf{x}_i) + i \cdot H_2(\theta) * I(\mathbf{x}_i)$.

Figure 1. Computation results of orientation selective filtering with different orientation fields. Top row shows a fingerprint with correct orientation field, and the resulting filtered image contains only a few corner points, where most of the detected corner points correspond to true minutiae points. Bottom row shows the same fingerprint with all orientations equal to $3\pi/4$. The resulting filtered image contains a large number of corner points at place where the orientation disagrees with the ridge flow. Most of these detected corner points do not correspond to the true minutiae points.

The filtered image P can be interpreted as the result of fingerprint enhancement, which would be clean and smooth if the estimated orientation field O agrees with the true ridge flow orientation in the fingerprint image. Please see Figure 1 for an example. Therefore, we can justify that quality of orientation field $O(\mathbf{x}_i)$ can be interpreted by counting the number of corner points $S(\theta, \mathbf{x}_i)$ appearing in the window $W(\mathbf{x}_i)$ of the filtered image P. The corner points on P are detected by Harris corner detector [16]. The computation is denoted as follows:

$$S(\theta, \mathbf{x}_i) = \sum_{\mathbf{x}_i \in W(\mathbf{x}_i)} \delta(det(A(\mathbf{x}_i)) - \kappa \cdot trace^2(A(\mathbf{x}_i)) > c), \tag{7}$$

where $\delta(det(A(\mathbf{x}_i)) - \kappa \cdot trace^2(A(\mathbf{x}_i)) > c)$ is 1 if $\delta(det(A(\mathbf{x}_i)) - \kappa \cdot trace^2(A(\mathbf{x}_i)) > c$ and 0 otherwise. A denotes the partial derivative of P:

$$A = \sum_{\mathbf{x} \in W} \begin{bmatrix} P_x^2(\mathbf{x}) & P_x(\mathbf{x})P_y(\mathbf{x}) \\ P_x(\mathbf{x})P_y(\mathbf{x}) & P_y^2(\mathbf{x}) \end{bmatrix}. \tag{8}$$

The two constants κ and c are empirically determined, and we found that good results are obtained with the setting $\kappa = 0.04$ and $c = 2$. We also note that $S(\theta, \mathbf{x}_i)$ can be evaluated efficiently by using the technique of integral image proposed by Viola et al. [17].

Finally, the mathematical formulation of the single quality potential function $\phi_i^q(O(\mathbf{x}_i))$ can be expressed as an affinity measurement in the following form:

$$\phi_i^q(O(\mathbf{x}_i)) = \exp(\frac{-S(O(\mathbf{x}_i), \mathbf{x}_i)^2}{2\sigma_q^2}). \tag{9}$$

Let $\tilde{\theta} \in [0, \pi]$ denote the angle between the two orientations $O(\mathbf{x}_i)$ and $O(\mathbf{x}_j)$. The pairwise consistent potential function $\psi_{ij}^c(O(\mathbf{x}_i), O(\mathbf{x}_j))$ can be expressed as an affinity measurement in the following form:

$$\psi_{ij}^c(O(\mathbf{x}_i), O(\mathbf{x}_j)) = \exp(\frac{-\tilde{\theta}^2}{2\sigma_c^2}). \tag{10}$$

The model parameters σ_q and σ_c control the sensitivity of the potential functions, and can be chosen by cross validation. Good results are obtained with the setting $\sigma_q = 1$ and $\sigma_c = 2.5$.

3.3. Efficient Discrete MRF Representation

So far we have introduced an MRF that represents a joint probability distribution over the continuous orientation variables O. In practice, it is more difficult, less accurate, and less efficient to perform inference in the continuous space. Therefore, in this subsection, we propose how to discretize the continuous orientation space by using training fingerprint examples.

Henry [18] has proposed a fingerprint classification scheme that divides fingerprints into five common classes, such as arch, tented arch, left loop, right loop, and whorl.

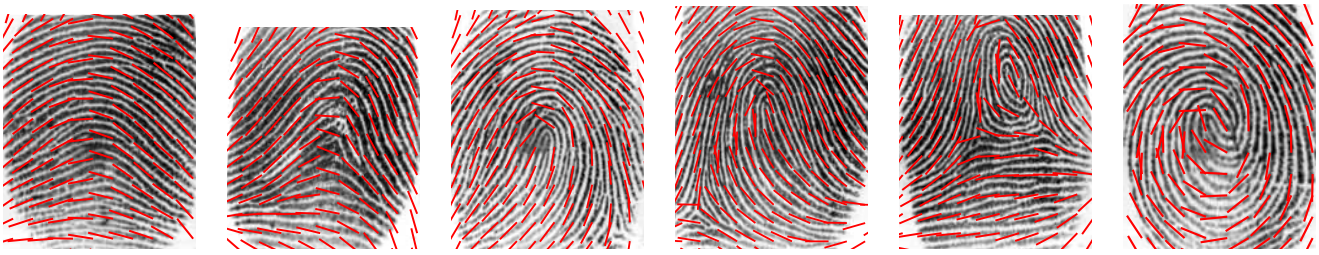

Figure 2. Six commonly used fingerprint classes: arch, tented arch, left loop, right loop, central pocket whorl, and twin loop whorl. The orientation fields are denoted by red arrows. Our training set contains two images from each class.

Figure 2 depicts these classes. We notice that the orientation fields of two fingerprints will be similar if they belong to the same class. Therefore, we collect a set of N high quality fingerprint images from different classes as training examples. For a given test fingerprint, we first initialize the orientation field of the test fingerprint by a traditional gradient-based approach in [9], and then align the orientation fields between the test fingerprint and the N training fingerprints by a standard approach of affine registration [19, 20]. After the alignment process, we collect a candidate set $\mathcal{C}_{\mathbf{x}_i} = \{c_j : j = 1 \dots N+1\}$ that includes the values c_j of the aligned orientation fields from the training fingerprints and the initialized value of the test fingerprint at every pixel location $\mathbf{x}_i$. Using the set $\mathcal{C}_{\mathbf{x}_i}$ we can discretize the domain of O, such that each value corresponds to a possible guess from the prior examples[1].

3.4. MRF Inference

Our goal is to find the posterior marginal probabilities of each variable $O(\mathbf{x}_i)$ in the discrete MRF described in Section 3.3. There are many existing algorithms for MRF inference. We choose loopy belief propagation (LBP) [21] in our framework, because LBP has been shown to perform well in a broad range of research works.

4. Experiments and Results

In this section, we describe experimental evaluations of our fingerprint orientation field estimation and fingerprint enhancement algorithms. The aim for these experiments is to demonstrate that ideas introduced in this paper enhance poor quality regions of fingerprint images and significantly improve the accuracy of a fingerprint verification system.

4.1. Data Acquisition and Parameter Setting

Fingerprint Verification Competition (FVC) organization periodically collects fingerprint databases for fingerprint algorithm evaluation [22, 23]. The databases are made available to the research community for benchmarking fingerprint algorithms. We seriously considered using these database in our evaluation but ultimately decided to use our own database for the following reason. The size of the FVC databases and number of fingerprint comparisons conducted according to the FVC protocol yields statistically significant results only up to False Acceptance Rate (FAR) of 0.1%. However, most commercial systems operate at 0.01% or lower FAR. In fact, we currently set our algorithm to operate at 0.001% FAR and plan to report results at 0.0001% FAR in the near future. Further, in consideration of commercial applications of fingerprint algorithms, we use an enrollment algorithm that requires multiple fingerprint images and performs a template consolidation during fingerprint enrollment. Finally, our protocol explicitly take template ageing into account by strictly requiring that verification fingerprint images be acquired no sooner than 6 weeks after the acquisition of fingerprint images for enrollment. Our internal dataset, acquired using commercial URU4000B optical fingerprint reader, meets these requirements. It contains fingerprint images from a total of 192 fingers in 48 users. We use typically four impressions per finger for enrollment and 24 impressions per finger (collected after 6 weeks but within a single sitting) for verification. Finally, we argue that the specific choice of dataset is not particularly critical in this work as long as it is large enough to yield statistically significant results since our goal is to demonstrate only the relative improvement in verification accuracy between our approach and the state-of-the-art (e.g., orientation diffusion approach [9]).

In our current implementation, the following parameter setting were found to be effective to obtain good experimental results. The size of the neighboring window W was set to 8, and $N = 12$ training examples were used to discretize the orientation fields for MRF inference.

The proposed framework is currently implemented in Matlab without any code optimization on a standard 2.0 GHz Intel Pentium (R) machine. The average process time for each fingerprint image in our proposed method is 30.2 seconds. We plan to improve this by orders of magnitude in our future work.

[1] A straightforward way is to quantize the orientation uniformly into N bins. This has been tested but the results are worse than the proposed approach.

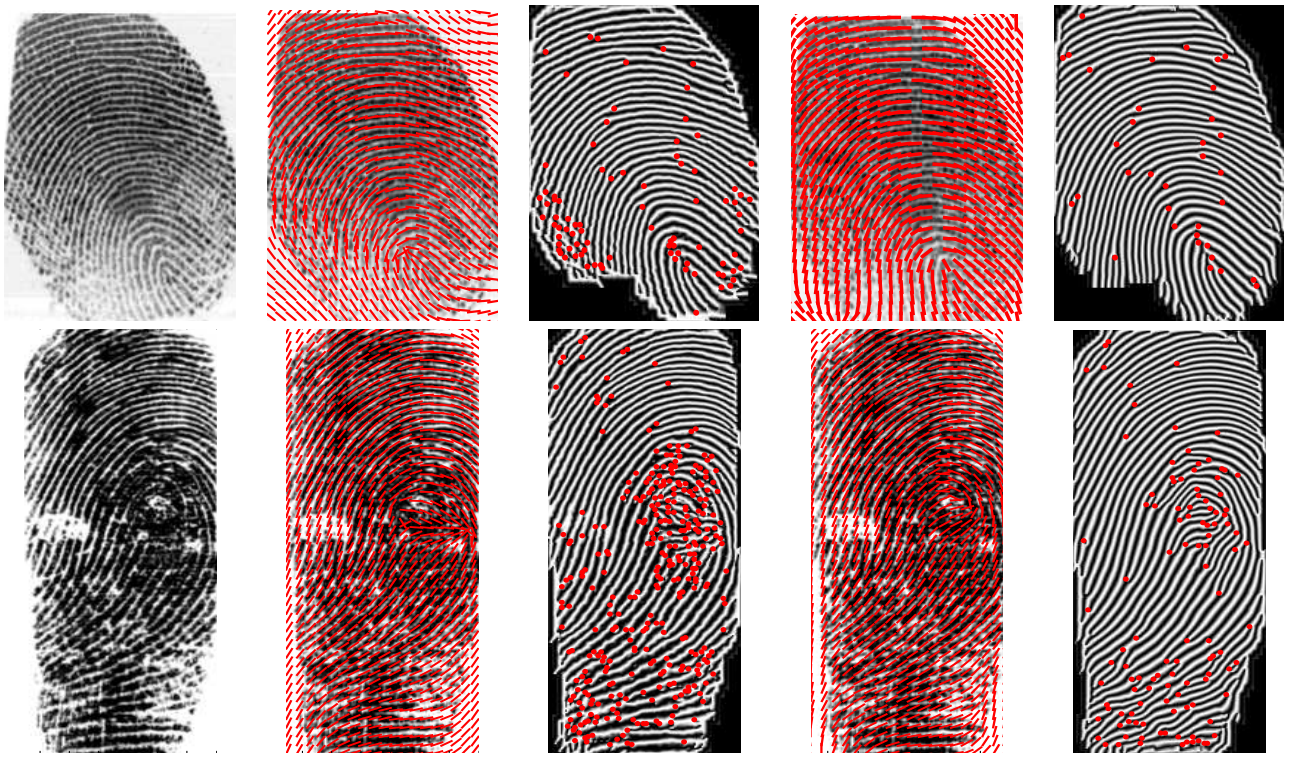

Figure 3. Qualitative results of fingerprint orientation estimation and enhancement. (1) Original fingerprint images. (2.a)-(2.b) Orientation fields and enhancement results produced by steerable filters with the orientation diffusion approach [9]. (3.a) - (3.b) Orientation fields and enhancement results produced by the proposed approach. Red arrows denote orientation fields, and red points denote detected corner points. Our approach results in fewer corner points that do not correspond to true minutiae points.

4.2. Qualitative Fingerprint Enhancement Results

Figure 3 displays the qualitative comparison on two fingerprint examples. Our orientation field estimation and enhancement results are shown in the fourth and fifth columns, respectively. In the second column we show the smooth orientation fields generated by the state-of-the-art orientation diffusion approach [9]. The enhancement results in the third column are obtained by using the orientation field of the second column and filtering the fingerprint image with the same steerable filters[2]. These comparisons demonstrate that our approach is capable of delivering precise fingerprint enhancement results under difficult noise conditions, including random sensor noise and structured noise (creases and scars).

4.3. Quantitative Fingerprint Verification Results

We have shown good results for visual inspection in the previous subsection. However, we are primarily interested in improving the accuracy of a fingerprint verification system. For this purpose, we conduct a goal-directed test keeping all the components the same except the orientation field estimation. We use a minutiae-matching algorithm that first aligns the verification minutiae set with the enrollment minutiae set using a gradient-based affine alignment [19, 20]. Correspondence between minutiae points are found during the alignment stage by using tolerance hyper-spheres. Finally the matching scores are computed as a function of the number of matching minutiae. On our dataset, we are able to perform more than 3 million imposter verification comparisons and thus have more than 30 errors at 0.001% FAR for statistical significance. Figure 4 shows the resulting receiver operating characteristic curve (ROC). Our proposed algorithm provides reasonable improvement along the entire ROC curve on our dataset. The False Rejection Rate (FRR) is almost halfed at an FAR of 0.001%, which indicates the strength of our proposed framework.

[2]Gabor filter can also be applied here, and the enhancement result looks similar.

5. Conclusion and Future Work

We have proposed a principled framework to compute orientation fields in fingerprint images by exploiting a small number of training examples of different fingerprint classes.

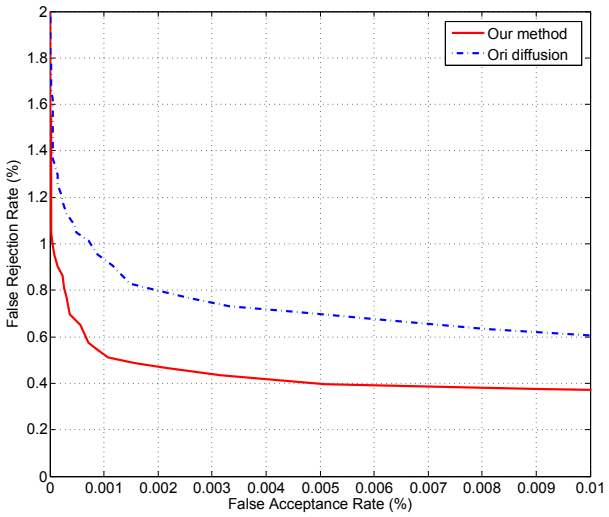

Figure 4. ROC comparison on our fingerprint dataset. The false acceptance rate (FAR) is plotted on the x-axis and the false rejection rate (FRR) is plotted on the y-axis. The ROC shows two curves; the red curve represents the performance of our proposed framework, and blue curve denotes the performance of the orientation diffusion approach [9].

We have demonstrated that our algorithm provides consistent improvement of fingerprint verification accuracy on a relatively large fingerprint dataset. In the future, we would like to increase our dataset to be able to estimate accuracy at 0.0001% FAR. The current implementation is computationally intensive because each test image needs to be aligned with each of the training examples. We are currently looking for a fast alignment algorithm as well as investigating alignment-free approaches.

There are many directions where this work can be extended. We would like to incorporate additional prior information such as singular points and creases in the proposed MRF framework. The current framework can enhance fingerprint ridge structures in noisy regions only when at least some part of the fingerprint image is good quality (to establish alignment with the training orientation fields). We will be looking at methods to make our method more robust to fingerprint images that do not have any good quality regions.

References

[1] L. Hong, Y. Wan, and A. Jain, "Fingerprint image enhancement: Algorithm and performance evalution," *IEEE Trans. Pattern Analysis and Machine Intelligence*, vol. 20, no. 8, pp. 777–789, 1998.

[2] R. Bolle S. Chikkerur, S. Pankanti and V. Govindaraju, "Minutiae verification in fingerprint images using steerable wedge filters," in *Indian Conf. on Computer Vision, Graphics & Image Processing*, 2004.

[3] M. Kass and A. Witkin, "Analyzing oriented patterns," *Computer Vision, Graphics and Image Processing*, vol. 37, no. 3, pp. 362–385, 1987.

[4] A. R. Rao and R. C. Jain, "Computerized flow field analysis: Oriented texture fields," *IEEE Trans. Pattern Analysis and Machine Intelligence*, vol. 14, no. 7, pp. 693–709, 1992.

[5] N. Ratha, S. Chen, and A. Jain, "Adaptive flow orientation based feature extration in fingerprint images," *Pattern Recognition*, vol. 28, pp. 1657–1672, 1995.

[6] A. Jain, L. Hong, and R. Bolle, "On-line fingerprint verification," *IEEE Trans. Pattern Analysis and Machine Intelligence*, vol. 19, no. 4, pp. 302–314, 1997.

[7] A. M. Bazen and S. H. Gerez, "Systematic methods for the computation of the directional fields and singular points of fingerprints," *IEEE Trans. Pattern Analysis and Machine Intelligence*, vol. 24, no. 7, pp. 905–919, 2002.

[8] Y. Wang, J. Hu, and F. Han, "Enhanced gradient-based algorithm for the estimation of fingerprint orientation fields," *Applied Mathematics and Computation*, vol. 185, no. 2, pp. 823–833, 2007.

[9] P. Perona, "Orientation diffusions," in *IEEE Trans. on Image Processing*, 1998, pp. 232–237.

[10] B. G. Sherlock and D. M. Monro, "A model for interpreting fingerprint topology," *Pattern Recognition*, vol. 26, no. 7, pp. 1047–1055, 1993.

[11] J. Zhou and J. Gu, "A model-based method for the computation of fingerprints' orientation field," *IEEE Trans. on Image Processing*, vol. 13, no. 6, pp. 821–835, 2004.

[12] J. Li, W-Y. Yau, and H. Wang, "Constrained nonlinear models of fingerprint orientations with prediction," *Pattern Recognition*, vol. 39, no. 1, pp. 102–114, 2006.

[13] S. C. Dass, "Markov random field models for directional field and singularity extraction in fingerprint images," *IEEE Trans. on Image Processing*, vol. 3, no. 10, pp. 1358–1367, 2004.

[14] Y. Wang, J. Hu, and D. Phillips, "A fingerprint orientation model based on 2d fourier expansion (fomfe) and its application to singular-point detection and fingerprint indexing," *IEEE Trans. Pattern Analysis and Machine Intelligence*, vol. 29, no. 4, pp. 573–585, 2007.

[15] W. T. Freeman and E. H. Adelson, "The design and use of steerable filters," *IEEE Trans. Pattern Analysis and Machine Intelligence*, vol. 13, pp. 891–906, 1991.

[16] C. Harris and M. Stephens, "A combined corner and edge detector," in *Proc. of the 4th Alvey Vision Conf.*, 1988, pp. 147–151.

[17] P.Viola and M.Jones, "Robust real-time object detection," *Int'l. J. Computer Vision*, vol. 57, no. 2, pp. 137–154, 2004.

[18] E. Henry, "Classification and uses of finger prints," *Routledge, London*, 1900.

[19] G. Hager and P. Belhumeur, "Efficient region tracking with parametric models of geometry and illumination," *IEEE Trans. Pattern Analysis and Machine Intelligence*, vol. 20, no. 10, pp. 1025–1039, 1998.

[20] J. Shi and C. Tomasi, "Good features to track," *Proc. IEEE Conf. on Computer Vision and Pattern Recognition*, pp. 593–600, 1994.

[21] J. Pearl, "Probabilistic reasoning in intelligent systems," *Morgan Kaufmann, San Francisco*, 1988.

[22] D. Maio, D. Maltoni, R. Cappelli, J. L. Wayman, and A. K. Jain, "Fvc2004: Third fingerprint verification competition," *Proc. Int'l Conf. on Biometric Authentication*, pp. 1–7, 2004.

[23] Fingerprint Verification Competition (FVC), "http://bias.csr.unibo.it/fvc2006/," .